SIMULATIONS OF MAGNETIC DYNAMICS IN IRON-COBALT FILMS

Ming Yan, J. Berezovsky, P. A. Crowell and C. E. Campbell

School of Physics and Astronomy
University of Minnesota
Minneapolis, Mn 55455, USA

1. INTRODUCTION

In this paper we present preliminary results of recent micromagnetic simulations of the magnetic dynamics of thin iron-cobalt films. Specifically we have simulated films of bcc $Fe_{1-x}Co_x$ grown on (100)GaAs, where x is very close to 0.5, systems which are also being studied experimentally in our lab using the polar magneto-optic Kerr effect (MOKE)[1]. This is a particularly interesting ferromagnetic system because it has a four-fold volume anisotropy and a two-fold anisotropy due to surface bonding and morphology.

Simulations have been completed on both circular disks and rectangles of thickness $10 - 20\ nm$ and lateral dimensions of the order of micrometers. Systems of this size will have several domains unless they are saturated by a very high applied field. Our results show that the presence of more than one domain produces a rich dynamical behavior.

The most commonly studied dynamical response of a ferromagnet has been ferromagnetic resonance (FMR). Magnetic moments are aligned by an applied magnetic field, and then the response of the magnetic moments to a weak, perpendicular tipping applied field is measured. The geometry is illustrated in the lower right panel of Fig. 6. The tipping field $\mathbf{h}(t)$ may be an rf field or a pulse of finite duration. In the former case, as one either sweeps the large applied field, or sweeps the frequency of the tipping field, a strong resonance is found at the uniform FMR frequency f_0 given in the case of isotropic films with applied and tipping field in the plane of the film by:

$$f_0^2 = \left(\frac{\gamma}{2\pi}\right)^2 [H_0 + (N_y - N_x)M_s]\,[H_0 + (N_z - N_x)M_s)]$$

where γ is the gyromagnetic constant, H_0 is the orienting magnetic field applied in the x direction, the plane of the film is the xy plane and thus z is perpendicular to the plane, M_s is the saturation magnetization, and N_α are the demagnetization factors

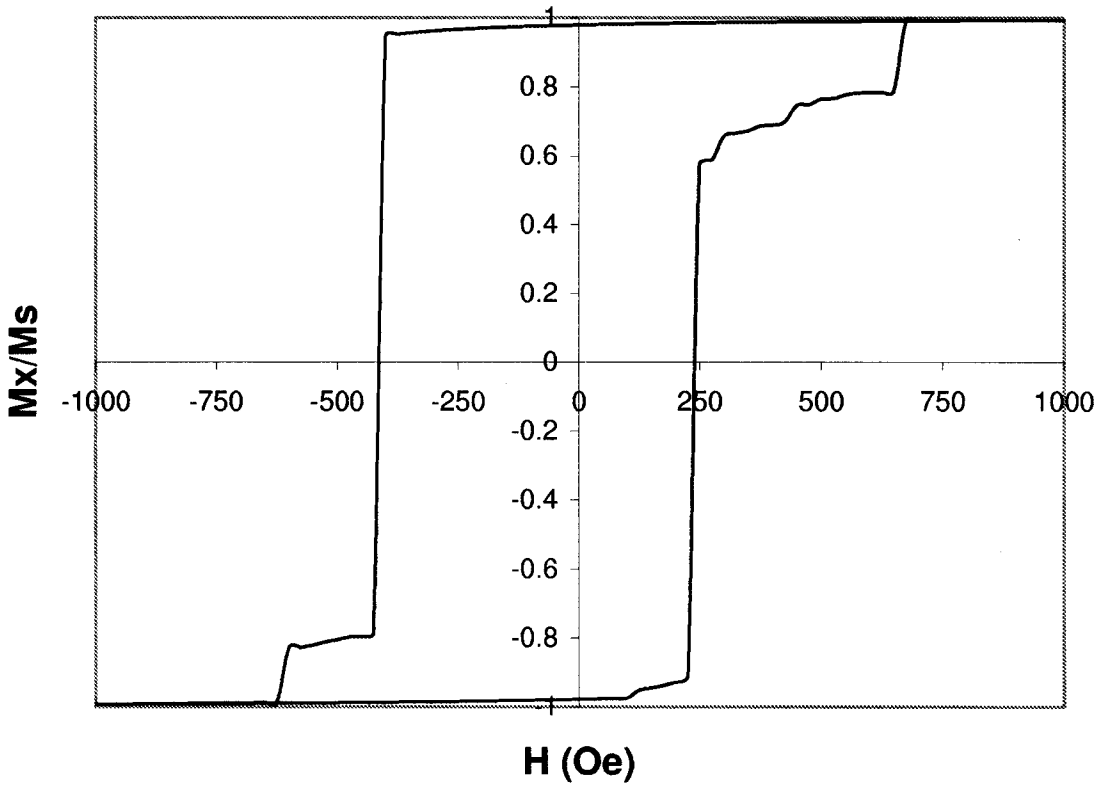

Figure 1. The hysteresis loop along the easy axis of the rectangular FeCo film described in the text and shown in Fig. 2. The magnetic field steps are of magnitude 25 Oe.

[2]. In this mode, all magnetic moments precess parallel to one another about their original direction. A time Fourier transform of the results of a pulsed tipping field will also reveal a strong response at this frequency, which however has the advantage that the Fourier transform of the time dependence of the response probes a wide spectrum of frequencies and thus reveals the location of other sharp resonances. These may then be probed by an rf tipping field. We use a combination of these methods in our simulations.

If the saturating field is in the plane of a thin film, the precession of each magnetic moment is slightly out of the plane, following an elliptical path around the original direction. This is a coherent rotation mode in the sense that all magnetic moments are parallel to each other. Thus it can be thought of as an infinite wavelength mode. In a film of finite dimensions, demagnetization due to the boundaries will have some effect on the ferromagnetic resonance mode, changing the frequency slightly from the value of f_0 given above. There will also be responses at other frequencies corresponding, e.g., to magnetostatic modes [3], spin wave modes [4], and/or to the multiple domain structure at moderate applied orienting fields.

As we will show below, our micromagnetic simulations of small systems show not only this ferromagnetic resonance, but also resonances at other frequencies which we show are associated with minority domains. As expected, we also see magnetic wave

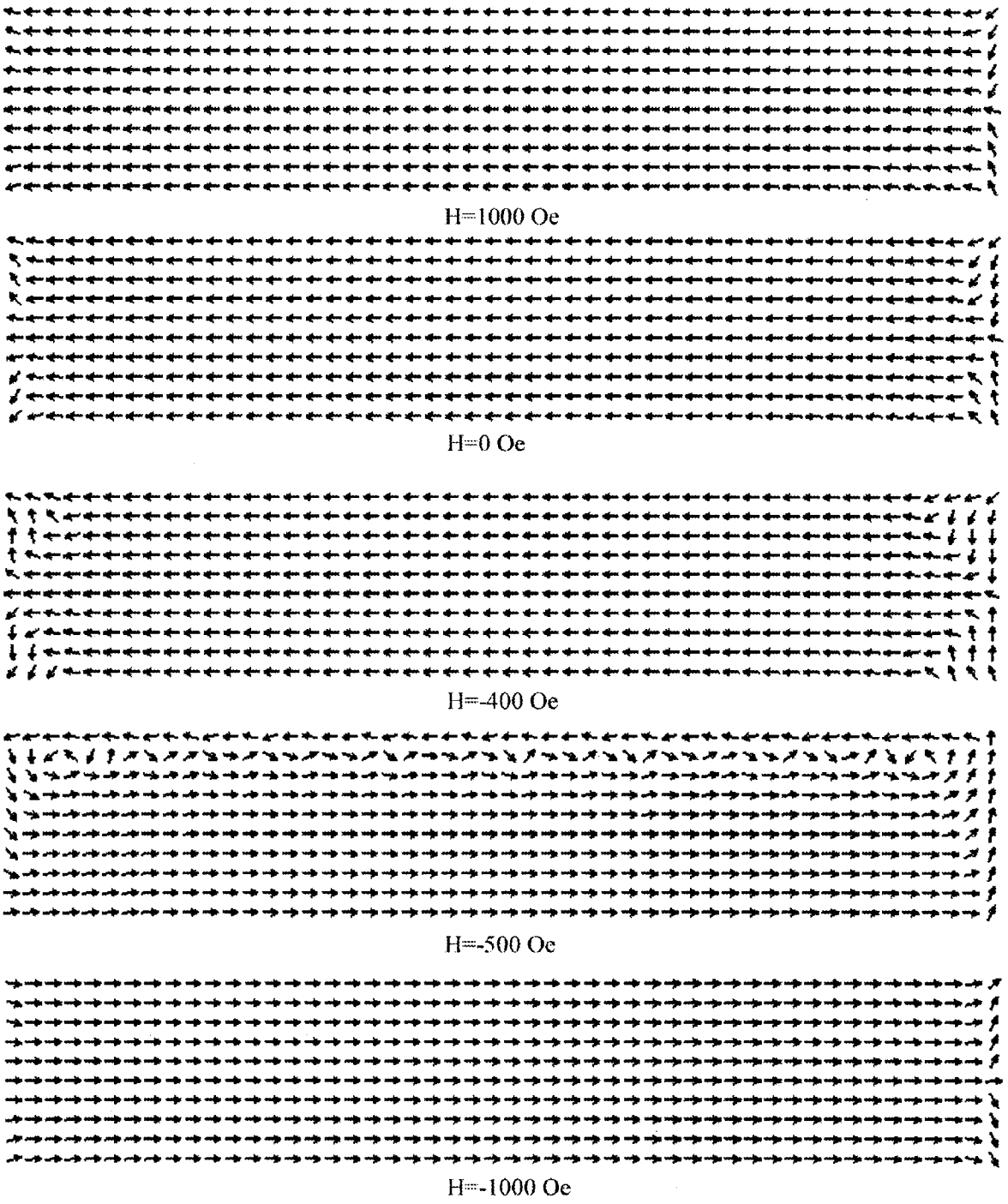

Figure 2. The magnetic structure of the rectangular FeCo film at four different applied fields during a simulated hysteresis loop along the easy axis, which is the horizontal axis in these figures. Each arrow represents 64 cells.

modes which are, however, difficult to analyze because of their complexity.

2. MICROMAGNETIC SIMULATIONS

The films were modeled by discretizing the system into cells of sufficiently small size that the structure of a domain wall may be easily resolved. For example, in the case of the rectangular films shown below, each cell was a cube 5 nm on a side.

The simulations were carried out by numerically solving the Landau-Lifshitz-Gilbert (LLG) equation of motion [5] for the directions of the magnetic moments, $\mathbf{m_i}$, of the individual cells comprising the film. The LLG equation is given by

$$(1+\alpha^2)\frac{d\hat{\mathbf{m}}_i}{dt} = -\gamma\hat{\mathbf{m}}_i \times \mathbf{H}_{eff,i} - \frac{\gamma\alpha}{M_S}\mathbf{m}_i \times (\mathbf{m}_i \times \mathbf{H}_{eff,i})$$

where $\hat{\mathbf{m}}_i$ is the unit vector in the direction of the magnetic moment of cell i, and the effective magnetic field $\mathbf{H}_{eff,i}$ in cell i is the sum of the applied field and four effective fields: the uniaxial anisotropy fields, the cubic anisotropy fields, the Heisenberg exchange fields due to the magnetic moments of nearest neighbor cells, and the dipolar field due to all of the other magnetic moments in the system:

$$\mathbf{H}_{eff,i} = \mathbf{H}_{ex} + \mathbf{H}_{u,i} + \mathbf{H}_{cu,i} + \mathbf{H}_{e,i} + \mathbf{H}_{d,i}$$

The uniaxial anisotropy effective field is given by:

$$\mathbf{H}_{u,i} = \frac{2K_u}{M_s} m_{i,x}\hat{\mathbf{x}}$$

The cubic anisotropy effective field is given by:

$$\mathbf{H}_{cu,i} = -\frac{2K_c}{M_s}[m_{i,x}(m_{i,y}^2 + m_{i,z}^2)\hat{\mathbf{x}} + m_{i,y}(m_{i,z}^2 + m_{i,x}^2)\hat{\mathbf{y}} + m_{i,z}(m_{i,x}^2 + m_{i,y}^2)\hat{\mathbf{z}}]$$

The effective exchange field is given by:

$$\mathbf{H}_{e,i} = \frac{2A}{M_s S^2}\sum_{n.n.j}\hat{\mathbf{m}}_j$$

where the sum is over nearest neighbor cells, and S is the length of the cubic cell side, in this case 5 nm. The constants entering these equations in the case of FeCo are $A = 10^{-6} erg/cm, M_s = 1900 emu/cm^3, K_c = 2.2 \times 10^5 erg/cm^3$, and $K_u = 2.4 \times 10^5 erg/cm^3$. Because we are most interested in the dynamics of the system, the Gilbert damping parameter α is chosen to be 0.01, which is in the range of ferromagnetic resonance measurements in typical metallic films.

3. SIMULATION RESULTS

Here we present some results of our simulations of two systems: A rectangular film of dimensions 2000 $nm \times 400$ $nm \times 10$ nm, and a disk of diameter 2000 nm and thickness 20 nm. The long direction of the rectangle is along the easy axis ([011] direction), corresponding to the x direction in the expression for f_0 (see the lower right panel in Fig. 6).

The hysteresis loop for the rectangle along the easy axis is shown in Fig. 1, and the corresponding magnetic moment configurations at five different fields along the top of the hysteresis loop are shown in Fig. 2. The initial saturating field is to the left. For ease of viewing the figures, only $1/64^{th}$ of the cells in the top layer are shown.

It is seen in the top panel of Fig. 2 that there is some non-uniformity in the magnetic moments in the first few columns at the left and right ends of the rectangle at an applied field of 1000 Oe, which is due to the effect of demagnetization which makes it energetically favorable for the moments to be aligned parallel to a nearby edge. An examination of this structure at higher resolution reveals that this non-uniformity is actually a set of domains, which shall be called "end zones", in each of the four corners of the rectangle. As the field is lowered and then reversed, these non-uniform regions expand inward from the ends. Note that most of the reversal of the magnetization occurs between -400 and -500 Oe. At -500 Oe, the reversal is almost completed except for the top rows.

The top/bottom asymmetry has to do with how one breaks the perfect metastability of an initial state which has top to bottom symmetry in a zero temperature dynamical simulation. This is a feature that is better explored in finite-temperature simulations. In the present case, the reversal of the bottom few rows happens just before the top rows. This is familiar from previous studies of permalloy-like films, including Monte Carlo simulations at finite temperatures[6]. It also accounts for the asymmetry of the hysteresis loop shown in Fig. 1, where the bottom branch of the loop begins at -1000 Oe, which is a state of magnetization that is slightly different than the original magnetization at +1000 Oe where the top branch of the loop begins.

We focus on the dynamics for the remainder of this paper. In Fig. 3 we show an example of magnetization reversal by tipping. The top panel in the figure is the equilibrium configuration for a horizontal field of -400 Oe on the top branch of the hysteresis curve; this panel also appears in Fig. 2. While in that state, a 10 Oe spatially uniform pulse in the plane of the film perpendicular to the majority magnetic moments is applied for 0.05 ns. In the next two panels of Fig. 3 one sees a reversal wall propagating from each end toward the center, leaving behind a complex region of rotating magnetic moments; the velocity of these fronts is of order 10^3 nm/ns. These fronts "collide" at approximately 1 ns, after which complex motion of the magnetism vectors ensues until it is damped to a final configuration in a few more nanoseconds [7]. This metastable state is not on the hysteresis curve, as can be expected because it has not been reached in a quasi-stable method.

The same tipping method may be used in other applied fields to weakly excite dynamical modes of the system as long as the applied magnetic field is not close to the coercive field [8]. An example is given in Fig. 4 and Fig. 5. Fig. 4 shows an FeCo

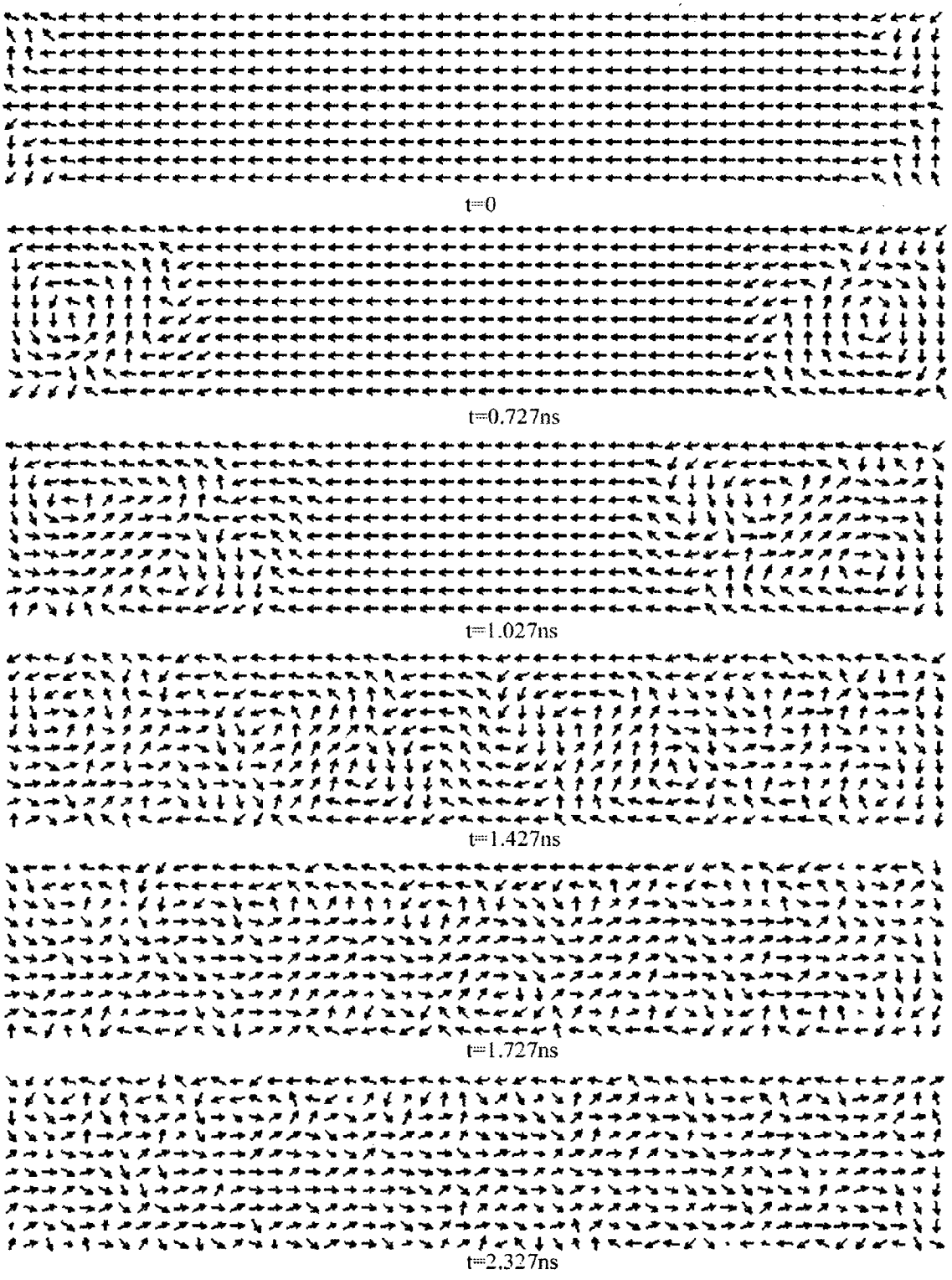

Figure 3. An example of a tipping induced reversal of the magnetization of a thin FeCo film in an orienting field of -400 Oe along the top branch of the hysteresis loop shown in Fig. 1. The elapsed time after the tipping pulse is indicated below each configuration.

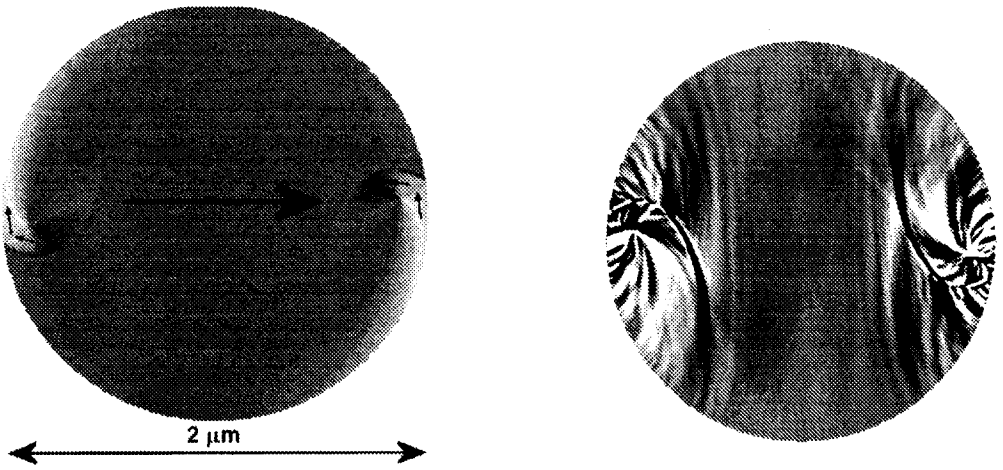

Figure 4. The results of a simulation of a $2\mu m$ disk equilibrated with an external horizontal magnetic field of 100 Oe. The image on the left is a black/white print of a false color image showing the planar projection of the direction of the magnetic moments. Most of the magnetic moments are horizontal, as indicated by the large arrow. The smaller arrows denote the magnetization directions near the horizontal diameter end points. The image on the right shows the z component of the magnetic moments of the disk displayed in a gray scale image, with white being the maximum positive value and black the maximum negative value, both much smaller than M_s.

disk of diameter $2\mu m$ in a horizontal field of 100 Oe. As described in the caption, the left-hand panel of this figure shows the predominant directions of the planar component of the magnetization, while the right-hand panel shows the magnetization components perpendicular to the plane of the film. While the out-of-plane component is much smaller than the in-plane component, a polar MOKE experiment is a sensitive measure of the former. Note the vortex-like magnetic moment configurations near the left and right edges of the film in the left panel of Fig. 4. This structure is to accommodate a change in the direction of the magnetic moments along the edge of the disk. The planar projection of the moments along the circumference of the film lie parallel to the edge of the film due to demagnetization. However the applied orienting field, which is horizontal in Fig. 4, prefers to align the moments to the right. Consequently, it is energetically most favorable for the planar components of the moments along the circular edge to be pointing clockwise along the edge in the top half of the disk, and counter-clockwise at in the bottom half. However, because the exchange interaction favors the parallel orientation of neighboring moments, this energetically costly at the points where the counter-clockwise direction runs into the clockwise direction, i.e., at the ends of the horizontal diameter near the vortex structure. The vortex structure accommodates this change from clockwise to counter-clockwise orientation with minimum energy. In the right-hand panel of Fig. 4 it is seen that, in these vortices, the components of the moments perpendicular to the disk have a complex, flower-like structure.

As in the case of the rectangle, a 10 Oe, $0.05ns$ pulse is applied to the disk in the plane along the hard direction, and the dynamics thereafter are tracked. In Fig. 5 one can follow these dynamics in the form of the z component of the magnetic moments. While the dynamical response is quite complicated, there are several obvious features.

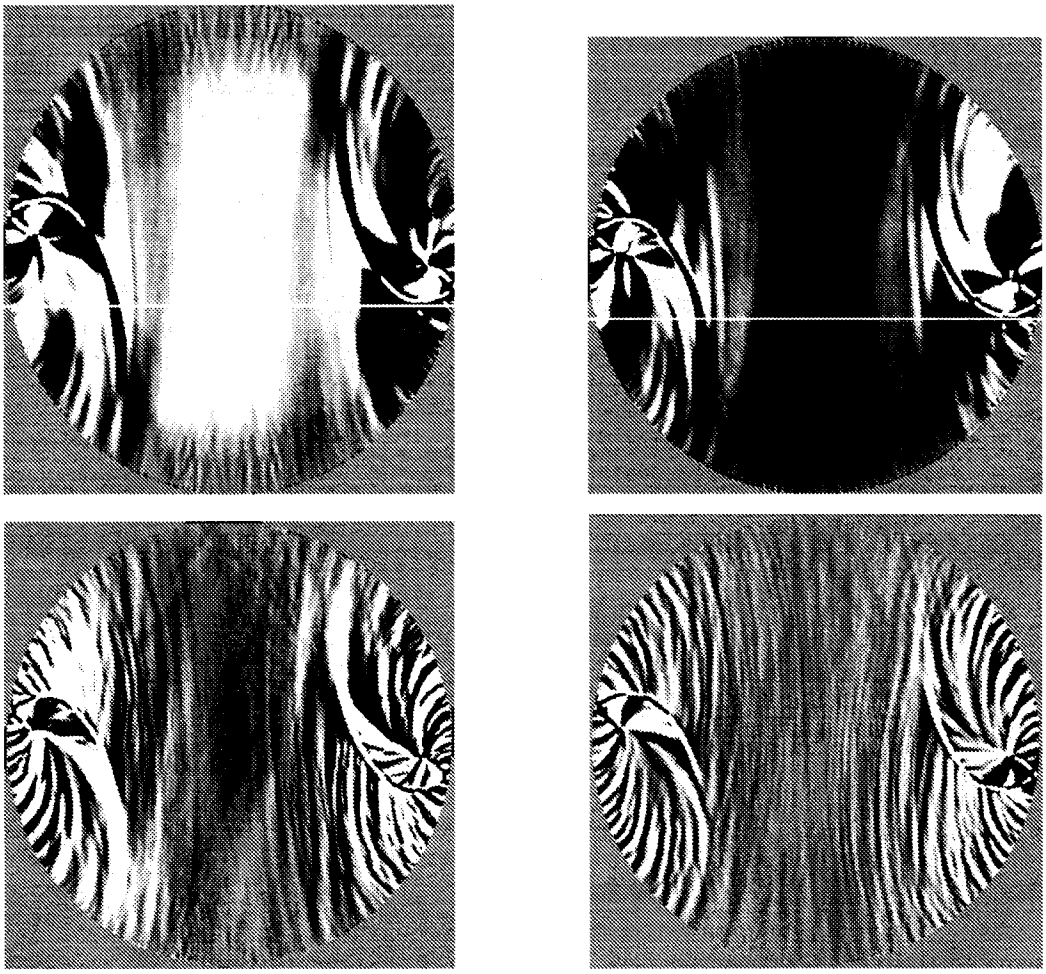

Figure 5. The z component of the magnetic moments of the disk shown in Fig. 4 after applying a pulsed tipping field as described in the text, displayed in a gray scale image, with white being the maximum positive value and black the maximum negative value, both much smaller than one. The first frame is 0.4 ns after the pulse, the next one (top right) is 0.45 ns after the pulse, then 1.50 ns, then 2.00 ns.

The central area of the film appears to be undergoing a coherent rotation during the period covered by the first two frames, which is the uniform FMR mode that occurs at $10GHz$ in this case. The top right panel is approximately one-half period after the top left panel. Much of the spatial distribution of the dynamical structure that ensues is tied to the two vortex regions that were evident in Fig. 4, or to the edges. There are also static or very long-lived structures seen as a flower petal pattern around each vortex. However, there are short wavelength modes that appear as ripples which begin near the edges of the circle and in the wings of the vortex structure. These ripples are moving across the film and also reflect from the edges to produce diagonal ripples. We believe that it is noteworthy that these modes are running waves that have their origins in the parts of the film where the equilibrium magnetization is non-uniform. Consequently the exchange interaction should play an important role, and most likely is the source of magnetic waves.

As time advances, the dynamics are damped by the damping term in the LLG

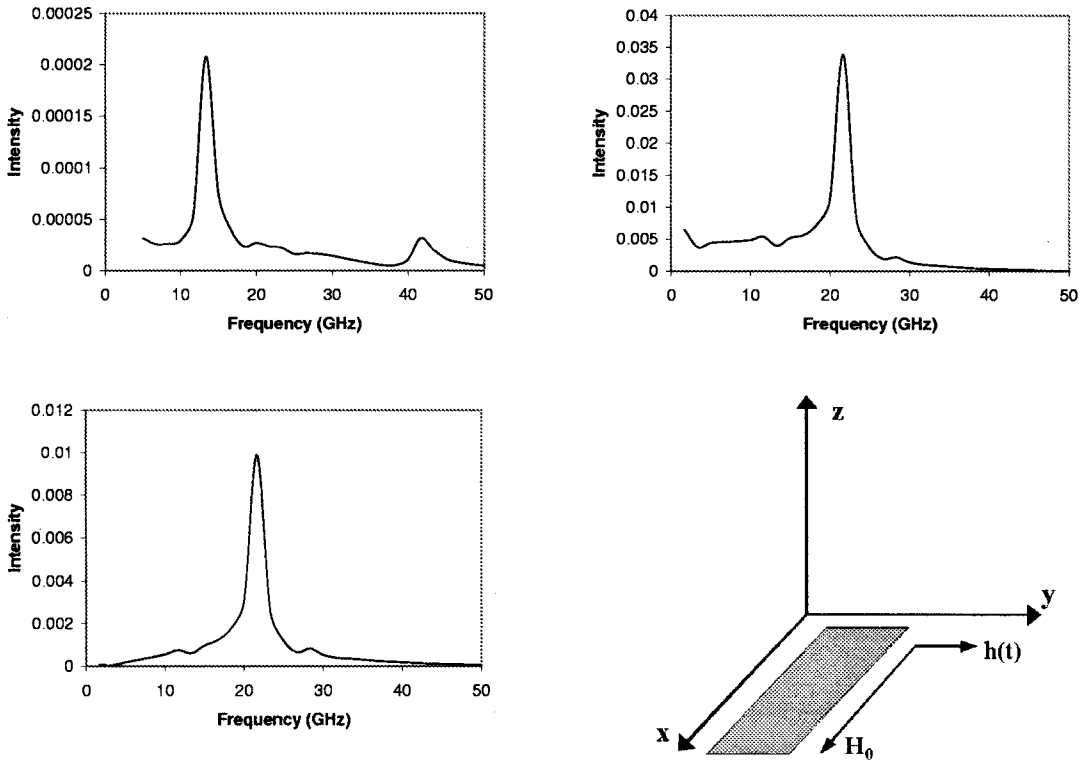

Figure 6. The frequency Fourier transform of the time dependence after a tipping pulse of the magnetization of a rectangular FeCo film in a horizontal orienting field of 1000 Oe, as shown in the top panel of Fig. 2 before the tipping pulse. The coordinate directions are given in the lower right panel, where $\mathbf{H_0}$ is the static, orienting field and $\mathbf{h}(t)$ is the tipping field. The upper left panel is for the x component of the magnetization, the upper right panel is the y component of the magnetization, and the lower left panel is the z component of the magnetization.

equation. But it appears that the FMR mode has in fact been damped by these magnetic waves before the latter are themselves damped out. Finally, it is clear that the damping is evolving the disk into a structure at long time which is very similar to the pre-pulse structure shown in Fig. 4.

Since some of this complex dynamics is precipitated by the regions of non-uniform magnetism at the boundaries, larger systems that have been prepared in minimally non-uniform states (i.e., without internal domain boundaries) should be less affected by modes that are spawned by the non-uniformity.

We have studied the frequency dependent response of the rectangle shown in Fig. 3 and 4 in much more detail. In that analysis, the simulations were done in a horizontal field of 1000 Oe in order to reduce the size of the end domains. This is the film shown in the top panel of Fig. 2. Thus one would expect a very clear FMR response from the interior of the system, away from the end regions. Note, however, that only one of every 64 magnetic moments is shown in that figure, thus the magnetic structure of the end zones is not completely revealed.

Fig. 6 shows the frequency responses of the three components of the total magnetization of the film. The fixed orienting field is in the x direction, the tipping field is applied in the y direction–both in the plane of the film–and the z direction is perpen-

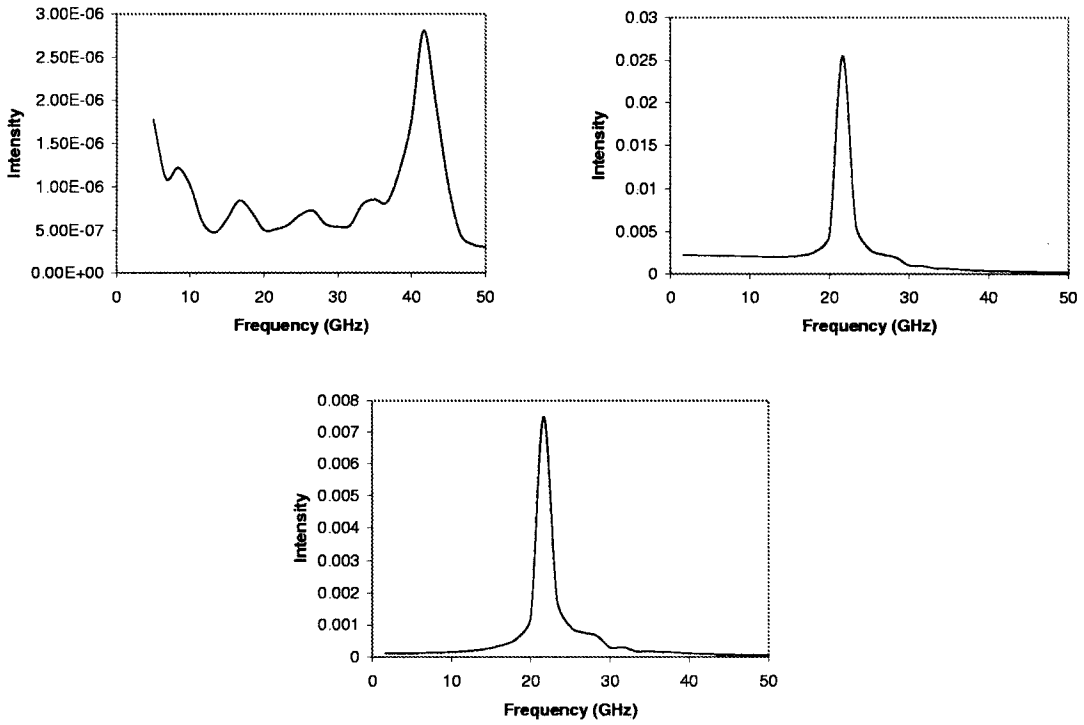

Figure 7. As in Fig. 6, but for a large region of the film midway between the left and right ends of the film, as discussed in the text. Note the difference in the vertical scales.

dicular to the plane of the film. The top right panel and the bottom left panel of Fig. 6 shows a strong resonance of the y and z components, respectively, at a frequency of approximately $21GHz$. This is very close to the mean-field frequency of $19GHz$ for an isotropic film of this geometry, given by the equation for the FMR frequency in Sec. 1. There is some additional structure at both low and high frequencies that we will discuss below. The top left panel of Fig. 6 shows that the strongest response of the x component of the total magnetization is at a frequency of $13GHz$, with a weaker response at $42GHz$. It should be noted that, with the orienting field in the x direction and the tipping field in the y direction, the ferromagnetic resonance in the x direction should be a very weak response showing up at twice the FMR frequency when the precession is elliptical, as it is in this case. That frequency corresponds to the smaller peak in the top left panel of Fig. 6.

To further elucidate the source of these resonances, we studied the dynamic response in two different regions of the film: the interior of the film well away from the end zones, so that the magnetic moments were parallel to one-another, and one of the corner regions in the end zones. The responses of the three magnetization components in the interior region are shown in Fig. 7. As expected, the x component (upper left panel) no longer has a response at $13GHz$, but it does have a weak resonance at $42GHz$. (At these very low intensities, no significance can be attributed to the lower frequency structure in the x component). Similarly, by far the strongest response of the y and z components (upper right panel and bottom panel, respectively) are at $21GHz$. Thus there is good evidence that the central part of this film is sustaining

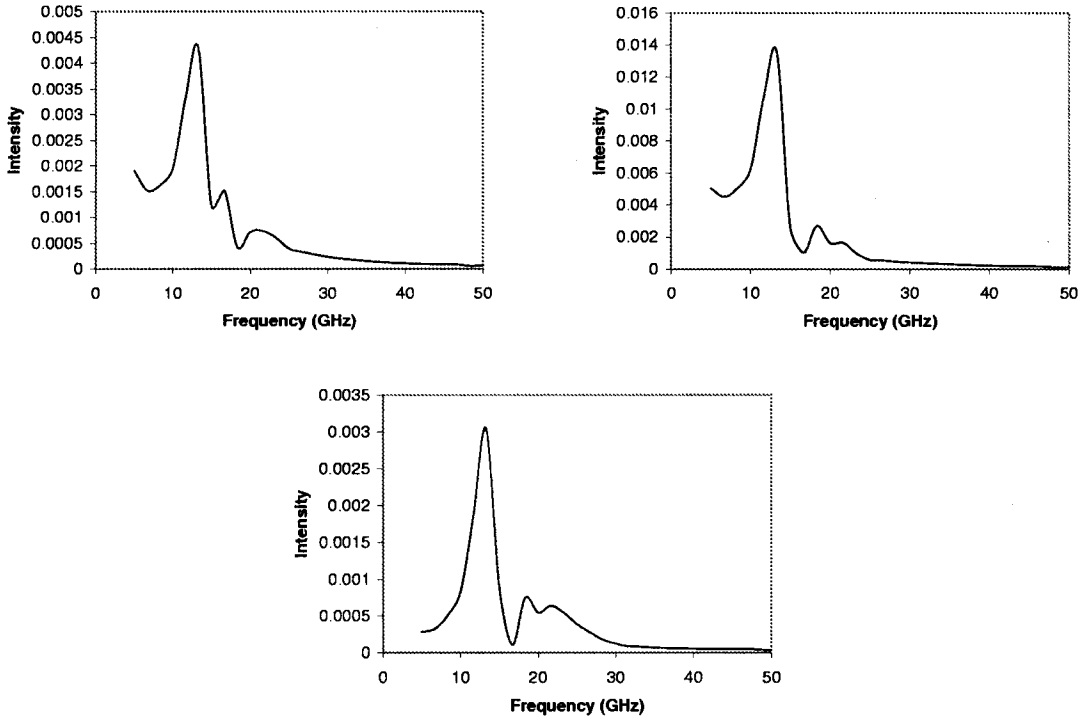

Figure 8. As in Fig. 6, but for a small region of the film near and encompassing a corner of the film where the magnetic moments are no longer in the x direction, as discussed in the text.

only an FMR mode.

Fig. 8 shows the results of the same analysis applied to one of the end zones. We hesitate to call this region a domain because the magnetic moments are nowhere aligned. Rather, this is a transition region between the horizontal orientation of the magnetic moments in the interior of the film and the magnetic moments at the ends of the film where there is a significant component parallel to the y or negative y direction in response to the demagnetization fields. In the top panel of Fig. 2, this is best seen on the right end, where the last shown column of magnetic moments is indeed the last column in the film, while at the left end one is actually seeing the eighth column in from the left end. Thus there are four end zones, one in the vicinity of each corner, extending from a corner to the middle of the left or right end. These regions are more like domain walls than domains. Each of the end zones is 200 nm in the y direction and a maximum of 50 nm in the x direction, with a boundary within the film that encloses the moments which are not parallel to the x direction. The analysis in Fig. 8 is for only one of these regions, each of which give the same results. The most notable feature of the panels in Fig. 8 is that it they clearly indicate that the $13GHz$ response seen in Fig. 6 but not in Fig. 7 is in fact located in the end zones. Given the splaying of the magnetic moments, it is not surprising that all three components respond at this frequency. There is additional structure at higher frequency that has not yet been fully analyzed. However, there is no peak at $26GHz$ that one would expect if the $13GHz$ resonance were a ferromagnetic resonance peak. Moreover, the fact that the magnetic moments are not parallel means that exchange

coupling should contribute significantly to the dynamics. We can speculate that some of this structure is due to magnetic waves at finite wavenumber. Indeed, we find that a cell-by-cell observation of the magnetization shows that there are in fact running waves involved in the motion of the magnetic moments. Finally, we note that the highest frequency structure is near $21GHz$ and thus might be an indication that the FMR resonance leaks into these end zones through their boundaries, which are in any case not well defined.

4. DISCUSSION AND CONCLUSIONS

We have reported preliminary results of micromagnetic simulations of the dynamics of micron sized thin FeCo films in a disk geometry and a rectangular geometry. This is motivated by time-resolved MOKE experiments on similar (but larger) FeCo films in our laboratory [1]. Ferromagnetic resonance is clearly seen in these simulations, but there is in addition more complex dynamics associated with edge regions where the magnetic moments are not fully aligned with the applied orienting field. Further analysis is necessary to completely explain these modes. A comparison with experiment must await simulations of larger films and/or experiments on smaller films.

ACKNOWLEDGMENTS

We wish to acknowledge the University of Minnesota Supercomputing Institute, the NSF through DMR-9983777 and the Alfred P. Sloan Foundation for partial support of this research, and the Army Research Office, Research Triangle Park, for partial support of travel through a grant to Southern Illinois University.

REFERENCES

[1] D. M. Engebretson, J. Berezovsky, J. P. Park, L. C. Chen, C. J. Palmstrom, and P. A. Crowell, accepted for publication, *J. Appl. Phys.*

[2] R. C. Handley, "Modern Magnetic Materials Principles and Applications," (John Wiley & Sons, New York, 2000).

[3] L. R. Walker, *Phys. Rev.* **105**, 390 (1957); R. W. Damon and J. R. Eshbach, *J. Phys. Chem. Solids* **19**, 308 (1961)

[4] M. H. Seavey, Jr., and P. E. Tannenwald, *Phys. Rev. Lett.* **1**, 168 (1958).

[5] E. D. Boerner and H. N. Bertram, *IEEE Trans. Mag.* **33**, 3052 (1997).

[6] A. Kunz and C. E. Campbell, *Cond. Matt. Theor.* **15** (2000).

[7] B. C. Choi *et al., Phys. Rev. Lett.* **86**, 728 (2001).

[8] W.K. Hiebert, A. Stankiewicz, and M.R. Freeman, *Phys. Rev. Lett.* **79**, 1134 (1997).